

Numerical simulation of the efficiency of quantum NOT operation on one superconducting flux qubit

¹Wu Tao (吴涛), ¹Liu Jian-she (刘建设), ²Li Zheng (李政)

¹Institute of Microelectronics, Tsinghua University, Beijing 100084

²Department of Electronic Engineering, Tsinghua University, Beijing 100084

Superconducting flux qubits are promising candidates for the building blocks of a quantum computer, which are essentially effective two-level systems. Flux qubits can be manipulated with magnetic flux microwave pulses which induce Rabi oscillations between the ground state and first excited state. However, microwaves will irradiate the qubit into non-computational states like the second and third excited states, and this probability may accumulate to cause errors if the operation time is long. Based on the wave functions of the qubit computed by the imaginary time evolution method, we numerically simulate the efficiency of quantum NOT operation upon one flux qubit through Rabi oscillations. In addition, it is revealed that the Gaussian-shaped pulse is beneficial to inhibit the leakage effect.

PACS number(s): 74.50.+r, 03.67.Lx, 85.25.Cp

Superconducting qubits [1, 2] are solid-state macroscopic systems conforming to the principles of quantum mechanics at ultra low temperatures. They can be compatibly fabricated in a large scale in a microelectronic process line and easily manipulated within circuits by microwave currents or flux pulses, which make them promising candidates for the building blocks of a quantum computer in the future [3]. In this family, superconducting flux qubits [4-10] utilize external magnetic flux as the convenient parameter to mark and control their eigenstates, which are insensitive to

background charge fluctuations but relatively fragile to magnetic flux noise compared to superconducting charge [11, 12] and phase [13, 14] qubits. Quantum superposition in the spectroscopy [6] and Rabi oscillations of one flux qubit in the time domain [7] have been observed. On the other hand, leakage effects of flux qubits has received relatively less observation [15] so far while the same effect of the phase qubit have been discussed before [14, 16].

In this letter, we compute the eigenstates of a single flux qubit using imaginary time evolution method [17-20]. Then based upon the results, under microwave magnetic flux pulse operation we simulate the efficiency of the qubit as a two level system in a four level system considering the leakage effect.

A three-Josephson-junction flux qubit is composed of a superconducting loop interrupted by three Josephson junctions [4-6] as shown in Fig.1(A). Junctions 1 and 2 have equal areas while junction 3 is α ($0 < \alpha < 1$) times smaller, and the critical current for them are I_c , I_c and αI_c , respectively. The loop is biased by magnetic flux $f\Phi_0$, where $\Phi_0 = \frac{h}{2e}$ is the superconducting flux quantum. It can be reduced to a two-level system when f is in the vicinity of $\frac{n+1}{2}$ with n an integer. Neglecting the loop inductance, the Hamiltonian of the system can be written as [5]

$$H = \frac{1}{2} \vec{p}^T \bullet M^{-1} \bullet \vec{p} + E_J [2 + \alpha - \cos(\varphi_1) - \cos(\varphi_2) - \alpha \cos(2\pi f + \varphi_1 - \varphi_2)], \quad (1)$$

where $M = C_J \left(\frac{\Phi_0}{2\pi} \right)^2 \begin{pmatrix} 1+\alpha & -\alpha \\ -\alpha & 1+\alpha \end{pmatrix}$, $\vec{p} = M \vec{\varphi}$, i.e., $\begin{pmatrix} p_1 \\ p_2 \end{pmatrix} = M \begin{pmatrix} \dot{\varphi}_1 \\ \dot{\varphi}_2 \end{pmatrix}$ and $E_J = \frac{I_c \Phi_0}{2\pi}$ is the Josephson energy for junction 1 and 2. For simplicity we take $f = f_x + \frac{1}{2}$ below, and Eq. (1) can be expressed explicitly as

$$H = \frac{(1+\alpha)}{2(1+2\alpha)C_J} \left(\frac{2\pi}{\Phi_0} \right)^2 (p_1^2 + p_2^2 + \frac{2\alpha p_1 p_2}{1+\alpha}) + E_J [2 + \alpha - \cos(\varphi_1) - \cos(\varphi_2) + \alpha \cos(2\pi f_x + \varphi_1 - \varphi_2)]. \quad (2)$$

It is different from the usual one like in Ref. 5 because the Hamiltonian remains in the

original frame without transformations. The potential of Eq. (2) is periodic in both dimensions and can be treated as repetitions of cells in the phase space. Fig. 1(B) shows one of such cells with a double-well in the centre.

In order to operate the qubit, we first have to compute the wave functions and energies of its eigenstates accurately. This is achieved by extending the fourth order imaginary time evolution method [17-20] to the two-dimension case. Replacing the one-dimensional fast Fourier transform (FFT) in [18] with two-dimensional FFT, we find that this method still works well.

The main idea of this method is to derive the wave functions of the lowest bound states of a system through damping the high energy components in the initial wave functions. First, choose a set of arbitrary wave functions [18], e.g., the wave functions of a two-dimensional harmonic oscillator as chosen in this work, ensuring that they contain enough frequency bandwidth. Then the wave functions are evolved in the imaginary time space under the operation of the Hamiltonian in Eq. (2) with the imaginary time unit $\varepsilon = i \bullet t$ substituting for t , when the components of the wave functions with high energies are exponentially damped with respect to that with low energies. Associated with the procedures of orthonormalizations, wave functions $\{\varphi_i(\vec{r})\}$ (with $i = 1, 2, \dots, n$) for the n lowest discrete energy levels can be filtered one by one. Then based upon the wave functions and the Hamiltonian, the energies of the eigenstates can be accurately obtained by integration.

Both α and f_x can be modulated to change the configurations of the eigenstates. In practice α is determined as long as the qubit is fabricated, therefore we shows the variation of the wave functions with f_x below. Table I illustrates the energies. Fig. 2 shows the ground states and the first excited states for $f_x = 0, -0.0002$ and -0.0050 respectively. Fig. 3 shows the second and third excited states $|2\rangle$ and $|3\rangle$ for $f_x = -0.0050$. We choose in the computation $\alpha = 0.80$, $E_J = 198.9437$ GHz and $C_J = 7.765$ fF.

Table I. The energies for the lowest four eigenstates with three values of f_x .

All the energies are in units of GHz.

f_x	E_0	E_1	E_2	E_3
0	316.1602	316.4915	345.1585	351.7933
-0.0002	316.0846	316.5671	345.1562	351.7953
-0.0050	311.9336	320.7190	343.8953	352.8491

The wave functions $|0\rangle$ and $|1\rangle$ for $f_x=0$ are symmetrical and anti-symmetrical, respectively, and they quickly lose the symmetry when f_x deviates from this degeneracy point. For the sake of readout, the currents in the loop for the two states should be set to circulate nearly oppositely, therefore we bias the qubit at $f_x=0.0050$, where the wave functions for $|0\rangle$ and $|1\rangle$ appear localized in two separate wells as shown in Fig. 2E and Fig. 2F.

Based on the results from the above part, we study the efficiency of quantum NOT operations upon one superconducting flux qubit with microwave magnetic flux pulse operations for the first time. The interaction of the microwave field with the qubit $W(t)$ is dealt with as a perturbation on the original Hamiltonian in Eq. (2) through an external microwave magnetic flux perturbation $f_\mu(t)\cos(\omega_0 t)\Phi_0$ on the flux bias $\left(f_x + \frac{1}{2}\right)\Phi_0$ through the loop, i.e.,

$$\begin{aligned}
W(t) = & \alpha E_J \cos[2\pi f_x + \varphi_1 - \varphi_2 + 2\pi f_\mu(t) \cos(\omega_0 t)] \\
& - \alpha E_J \cos(2\pi f_x + \varphi_1 - \varphi_2) \\
\cong & -\alpha E_J \sin(2\pi f_x + \varphi_1 - \varphi_2) \bullet 2\pi f_\mu(t) \cos(\omega_0 t) \\
= & F(t) \sin(2\pi f_x + \varphi_1 - \varphi_2),
\end{aligned} \tag{3}$$

where

$$F(t) = -2\pi\alpha E_J f_\mu(t) \cos(\omega_0 t), \tag{4}$$

$f_\mu(t)$ describes the amplitude of the external microwave magnetic flux pulse with $f_\mu(t) \ll f_x + \frac{1}{2}$ and ω_0 is the resonant angular frequency with $\hbar\omega_0 = E_1 - E_0$.

In the Hilbert space spaned by the eigenstates $|0\rangle$, $|1\rangle$, $|2\rangle$ and $|3\rangle$, the interaction $W(t)$ can be written as a 4×4 matrix with

$$W(t)_{i,j} = F(t) \langle i-1 | \sin(2\pi f_x + \varphi_1 - \varphi_2) | j-1 \rangle, \quad (5)$$

where $i, j = 1, 2, 3, 4$. The integration elements have been computed numerically, with which $W(t)$ is written as

$$W(t) = F(t)M, \quad (6)$$

where

$$M = \begin{bmatrix} -0.8806 & -0.0339 & -0.0036 & 0.0616 \\ -0.0339 & 0.8803 & 0.0592 & -0.0159 \\ -0.0036 & 0.0592 & -0.4216 & 0.4795 \\ 0.0616 & -0.0159 & 0.4795 & 0.3344 \end{bmatrix}. \quad (7)$$

From now on, we denote by $\hbar\omega_0$ the energy unit and by $\tau = \omega_0 t$ the time unit, and choose E_0 as the zero point measuring the energies. Then $F(t)$ is replaced by $F(\tau)$ with

$$F(\tau) = K(\tau) \cos(\tau), \quad (8)$$

$$K(\tau) = -2\pi\alpha f_\mu(\tau) \frac{E_J}{\hbar\omega_0}. \quad (9)$$

To achieve a NOT gate in the computational space or the population inversion between the ground state and the first excited state, the effective matrix element is just $M_{1,2}$ and $M_{2,1}$, where $M_{1,2}$ and $M_{2,1}$ is just the (1,2) and (2,1) elements in Eq. (7) -0.0339. To meet the requirement, the phase shift of the qubit under the pulse operation should just be π , i.e.,

$$\int_0^{\tau_p} K(\tau) M_{1,2} d\tau = \pi, \quad (10)$$

where τ_p is the duration of the pulse and If the magnetic flux pulse has the hard

pulse shape, then the pulse can be expressed as $f_\mu(\tau) = \frac{K_0 \hbar \omega_0}{-2\pi\alpha E_J}$ (for $0 \leq \tau \leq \tau_p$),

where $K_0 = K(\tau) = \frac{\pi}{\tau_p M_{1,2}}$. Here τ_p can be modulated. Figs. 4A and 4B illustrate the

Hard pulse and the Gaussian shaped pulse configurations with $\tau_p = 100$ and $\tau_p = 200$, respectively. If the Gaussian-shaped pulse is employed, then to meet the requirement of Eq. (10) one has

$$K(\tau) = \frac{\pi}{M_{1,2}} \frac{1}{\sqrt{2\pi\tau_w}} \exp\left(-\frac{(\tau - \frac{\tau_p}{2})^2}{2\tau_w}\right), \quad (11)$$

for $0 \leq \tau \leq \tau_p$. In Eq. (11) τ_w is the characteristic width of the Gaussian pulse chosen between $0.167\tau_p$ and $0.100\tau_p$.

The Hamiltonian of the system before the application of the microwave pulse is described by a 4×4 matrix, i.e.,

$$H_0 = \frac{1}{\hbar\omega_0} \begin{bmatrix} 0 & 0 & 0 & 0 \\ 0 & \hbar\omega_0 & 0 & 0 \\ 0 & 0 & E_2 - E_0 & 0 \\ 0 & 0 & 0 & E_3 - E_0 \end{bmatrix}, \quad (12)$$

where the energy level of the ground state is set to zero. The time-dependent Hamiltonian for the system is just $H_t = H_0 + W(\tau)$. Suppose that the qubit is described by the 4×4 density matrix $\rho(\tau)$, and the element (i,i) in the density matrix ρ denotes the probability of the system in state $|i\rangle$. The qubit stays in the ground state before the external magnetic flux irradiation, with

$$\rho(\tau=0) = \begin{bmatrix} 1 & 0 & 0 & 0 \\ 0 & 0 & 0 & 0 \\ 0 & 0 & 0 & 0 \\ 0 & 0 & 0 & 0 \end{bmatrix}. \quad (13)$$

The evolution of the density matrix is described by Liouville equation, i.e.,

$$i \frac{\partial \rho(\tau)}{\partial \tau} = [H_t(\tau), \rho(\tau)]. \quad (14)$$

Choosing a time step small enough ($\Delta \tau \approx 10^{-4} \sim 10^{-7}$), we can simulate the system by iterations as

$$\rho_{k+1} = \rho_k - i[(H_t)_k, \rho_k] \Delta \tau. \quad (15)$$

Tables II and III show the efficiency of the NOT gate versus the pulse durations.

Table II. The populations of the lowest four levels after the microwave magnetic flux irradiations with Hard-shaped pulses.

	$\tau_p = 100$	$\tau_p = 200$	$\tau_p = 400$
P0	0.2065	0.0139	4.2453e-4
P1	0.7898	0.9859	0.9996
P2	0.0033	1.3342e-4	9.5940e-6
P3	4.6247e-4	4.1095e-5	1.1245e-5

Table III. The populations of the lowest four levels after the microwave magnetic flux irradiations with Gaussian-shaped pulses.

	$\tau_p = 100$	$\tau_p = 200$	$\tau_p = 400$
P0	0.1160	0.0139	0.0114
P1	0.8402	0.8598	0.9886
P2	0.0209	3.4246e-4	0
P3	0.0228	7.3074e-4	0

In the simulations, $\Delta \tau = 2\pi$ corresponds to $\Delta t = \frac{2\pi}{\omega_0} \approx 0.1138\text{ns}$. It is found that sufficient operation time durations are required to obtain ideal population inversion between states $|0\rangle$ and $|1\rangle$, while suppressing the leakage to states $|2\rangle$ and $|3\rangle$.

However, in practice because of the existence of decoherence it is very demanding to perform an operation within a short time duration, then in a sense the Hard pulse is efficient enough compared to Gaussian pulse as shown in Table II and III. Nevertheless, if the leakage effect is more serious especially when coupled qubits are concerned, Gaussian shaped pulses or other pulses may be desirable although it is not as convenient as the Hard pulse to be generated.

In conclusion, utilizing the imaginary time evolution method we have accurately calculated the wave functions and energies for the eigenstates of the flux qubit. Based on these results, the efficiency of the quantum NOT operations upon single flux qubit is simulated, where the leakage into the second and third excited states are taken into account. We find that the Hard shaped magnetic flux microwave pulses are efficient to achieve the NOT operation as long as the pulse duration is long enough, while the Gaussian shaped pulse may inhibit the leakage effect better.

We greatly appreciate the help of Philip R. Johnson and Frederick W. Strauch in University of Maryland when we applied the imaginary time evolution method. Stimulating discussions with Wang Ji-lin, Li Tie-fu, Chen Pei-yi, Yu Zhi-ping and Li Zhi-jian are gratefully acknowledged. This work is supported by the 211 Program of Nanoelectronics of Tsinghua University.

References

- [1] Yu. Makhlin, G. Schön, A. Shnirman, *Rev. Mod. Phys.* **73**, 357(2001).
- [2] M. H. Devoret and J. M. Martinis, *Quantum Information Processing* **3**, 163(2004).
- [3] M. A. Nielsen and I. L. Chuang, *Quantum Computation and Quantum Information*(Cambridge University Press, Cambridge, UK, 2000).
- [4] J. E. Mooij, T. P. Orlando, L. Levitov, Lin Tian, C. H. van der Wal, and S. Lloyd, *Science* **285**, 1036 (1999).
- [5] T. P. Orlando, J. E. Mooij, L. Tian, C. H. van der Wal, L. S. Levitov, S. Lloyd, and J. J. Mazo, *Phys. Rev. B* **60**, 15398(1999).
- [6] C. H. van der Wal, A. C. J. ter Haar, F. K. Wilhem, R. N. Schouten, C. Harmans,

T. P. Orlando, S. Loyd, and J. E. Mooij, *Science* **290**, 773 (2000).

[7] I. Chiorescu, Y. Nakamura, C. J. Harmans, and J. E. Mooij, *Science* **299**, 1869(2003).

[8] Y. S. Greenberg et al., *Phys. Rev. B* **66**, 214525 (2002).

[9] Y. S. Greenberg et al., *Phys. Rev. B* **66**, 224511 (2002).

[10] Y. S. Greenberg, *Phys. Rev. B* **68**, 224517 (2003).

[11] Y. Nakamura, Y. A. Pashkin, J. S. Tsai, *Nature* **398**, 768(1999).

[12] D. Vion, A. Aassime, A. Cottet, P. Joyez, H. Pothier, C. Urbina, D. Esteve, and M. H. Devoret, *Science* **296**, 886(2002).

[13] J. M. Martinis, S. Nam, J. Aumentado, and C. Urbina, *Phys. Rev. Lett.* **89**, 117901(2002).

[14] M. Steffen, J.M. Martinis, and I.L. Chuang, *Phys. Rev. B* **68**, 224518(2003).

[15] L. Tian, Ph. D. thesis, Massachusetts Institute of Technology(2002)

[16] M. H. S. Amin, *cond-mat*/0407080(2004).

[17] P. R. Johnson, F. W. Strauch, A. J. Dragt, R. C. Ramos, C. J. Lobb, J. R. Anderson, and F. C. Wellstood, *Phys. Rev. B* **67**, 020509(2003).

[18] J. Auer, E. Krotscheck and S.A. Chin, *J. Chem. Phys.* **115**, 6841(2001); E. Krotscheck et al., *International Journal of Modern Physics B* **17**, 5459(2003).

[19] K. Takahashi and K. Ikeda, *J. Chem. Phys.* **99**, 8680(1993).

[20] M. D. Feit, J. A. Flek, Jr., and A. Steiger, *J. Comput. Phys.* **47**, 412(1982).

Figure Captions

Fig. 1.

(A) The three-Josephson-junction qubit. The blue crosses denote the junctions, and C_{j1} , C_{j2} and C_{j3} are the equivalent capacitances of the junctions with $C_{j1} = C_{j2} = C_J$ and $C_{j3} = \alpha C_J$.

(B) Contour configuration for one cell of the potential with $\alpha = 0.80$ and $f_x = -0.005$ in units of GHz. The whole potential is accurately the repetition of such cells.

Fig. 2.

(A) ground state with $f_x = 0$;

(B) first excited state with $f_x = 0$;

(C) ground state with $f_x = -0.0002$;

(D) first excited state with $f_x = -0.0002$;

(E) ground state with $f_x = -0.0050$;

(F) first excited state with $f_x = -0.0050$.

Fig. 3.

(A) the second excited state with $f_x = -0.0050$;

(B) the third excited state with $f_x = -0.0050$.

Fig. 4.

(A) Configuration of Hard pulse with $\tau_p = 100$;

(B) Configuration of Gaussian shaped pulse with $\tau_p = 200$.

Fig. 5.

The inversion of population between the ground state and the first excited state after the operation of **(A)** the Hard and **(B)** the Gaussian shaped microwave magnetic flux pulse with $\tau_p = 400$.

The population of the second excited state after **(C)** a Hard and **(D)** a Gaussian shaped microwave magnetic flux pulse with duration of $\tau_p = 400$.

The population of the second excited state after **(E)** a Hard and **(F)** a Gaussian shaped microwave magnetic flux pulse with duration of $\tau_p = 400$.

Fig. 1A-B

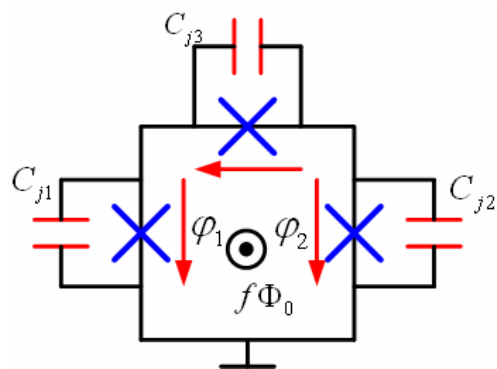


Fig. 1A

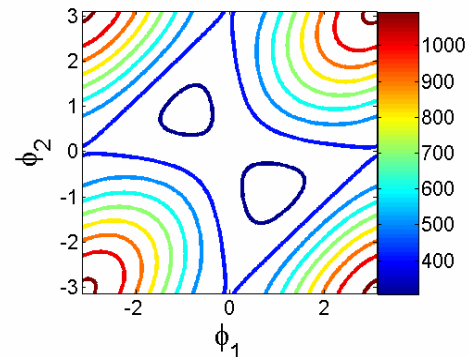


Fig. 1B

Fig.2A-F

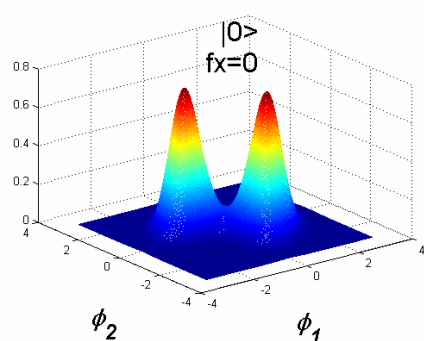


Fig. 2A

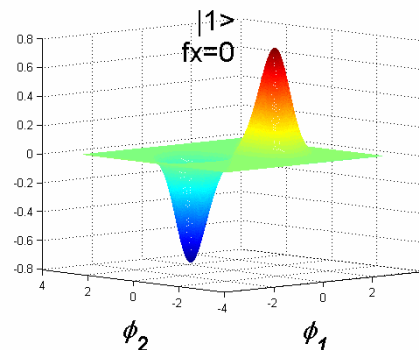


Fig. 2B

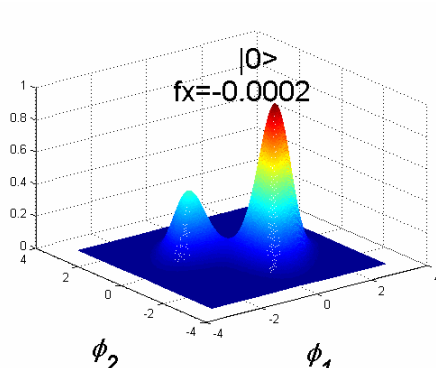


Fig. 2C

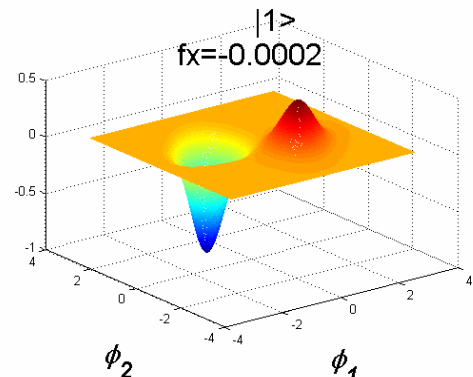


Fig. 2D

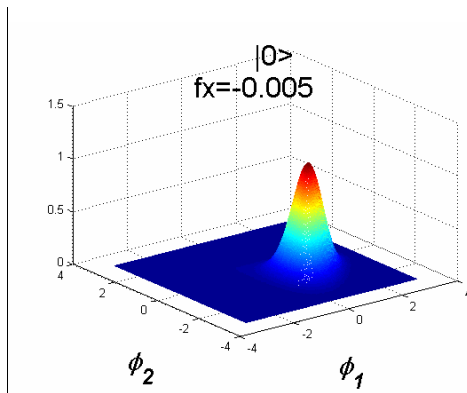


Fig. 2E

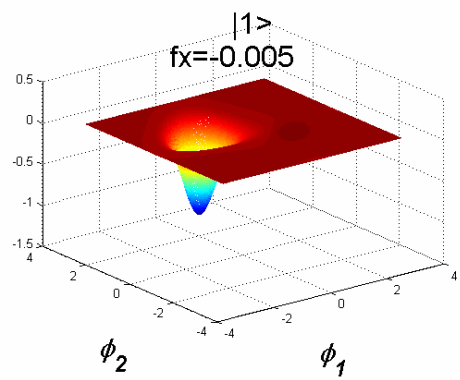


Fig. 2F

Fig. 3A-B

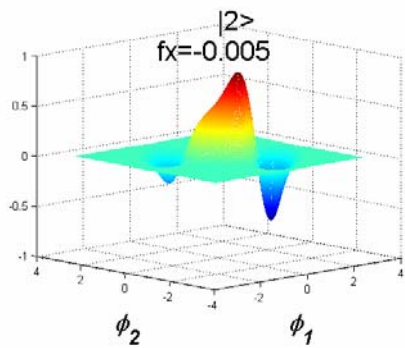


Fig. 3A

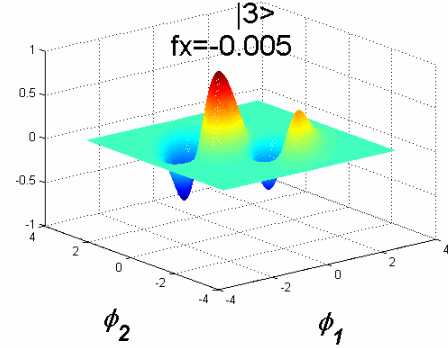


Fig. 3B

Fig. 4A-B

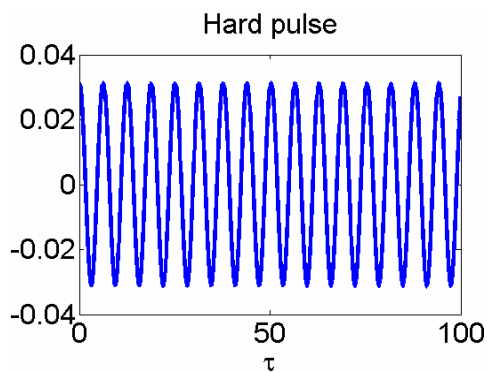


Fig. 4A

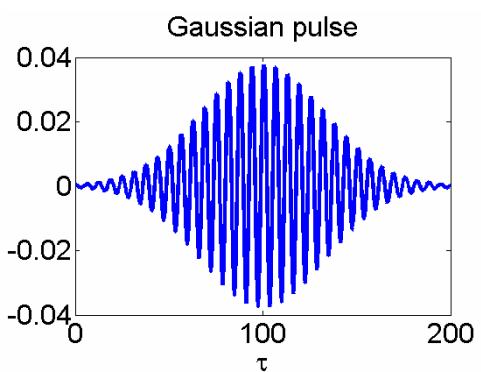


Fig. 4B

Fig. 5A-F

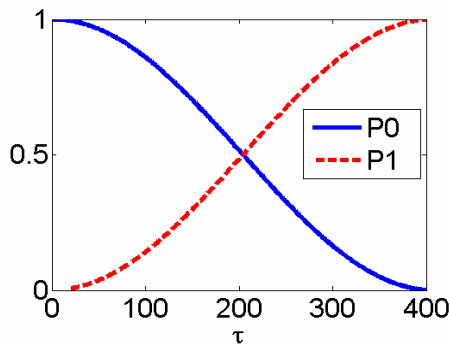


Fig. 5A

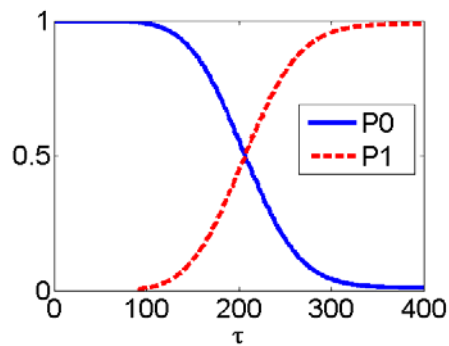


Fig. 5B

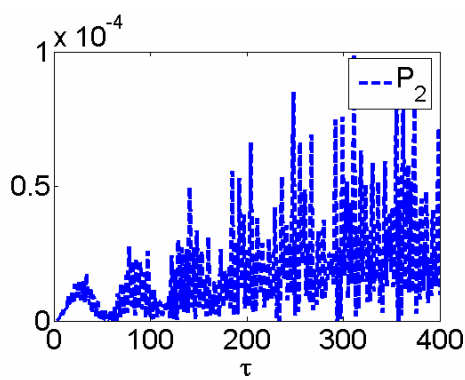


Fig. 5C

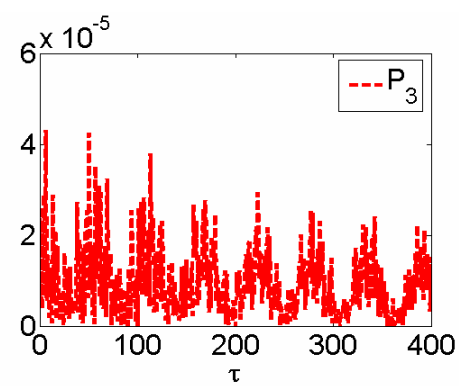


Fig. 5D

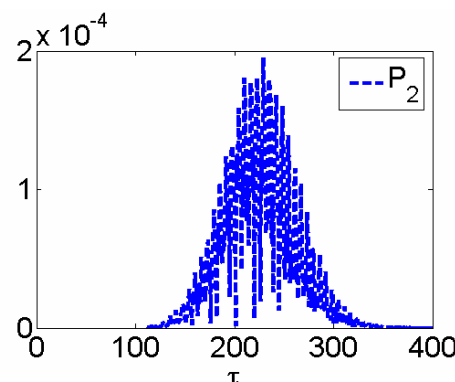


Fig. 5E

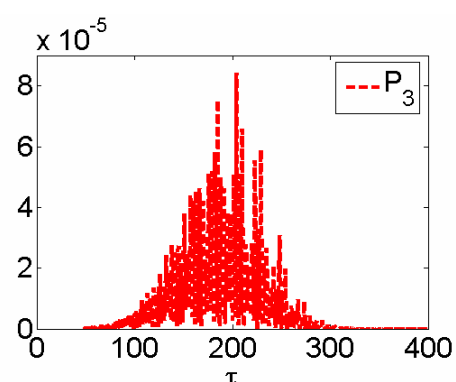


Fig. 5F